Targeted transfer of solitons in continua and lattices

H. E. Nistazakis,[1] P. G. Kevrekidis,[2] B. A. Malomed,[3] D. J. Frantzeskakis,[1] and A. R. Bishop[4]

[1]*Department of Physics, University of Athens, Panepistimiopolis, Zografos, Athens 15784, Greece*
[2]*Department of Mathematics and Statistics, University of Massachusetts, Amherst, Massachusetts 01003-4515*
[3]*Department of Interdisciplinary Studies, Faculty of Engineering, Tel Aviv University, Tel Aviv, Israel*
[4]*Center for Nonlinear Studies and Theoretical Division, Los Alamos National Laboratory, Los Alamos, New Mexico 87545*

We propose a robust mechanism of targeted energy transfer along a line, as well as on a surface, in the form of transport of coherent solitary-wave structures, driven by a moving, spatially localized external ac field ("arm") in a lossy medium. The efficiency and robustness of the mechanism are demonstrated analytically and numerically in terms of the nonlinear Schrödinger (NLS) equation, and broad regions of stable operation are identified in the model's parameter space. Direct simulations show that the driving arm can manipulate solitons equally well in a lattice NLS model. A salient feature, which is revealed by simulations and explained analytically, is a resonant character of the operation of the driving arm in the lattice medium, both integer and fractional resonances being identified. Numerical experiments also demonstrate that the same solitary-wave-transport mechanism works well in two-dimensional lattice media.

For dynamical models that can support solitary waves, an issue of obvious interest is a possibility to coherently transfer these localized pulses, especially in a targeted way, i.e., from an initial position to a prescribed final one. Systems in which this problem is important are ubiquitous (see e.g., Refs. [1,2]) in various areas, from bioenergetics to optics, and from catalytic reactions to nanoscale condensed matter physics.

Related problems were addressed in a number of recent studies. In particular, a laser beam was used in Ref. [3] (see also references therein) to locally modify the catalytic activity on a reaction surface, resulting in pulling reaction fronts coherently by the laser beam, or guiding the front inside a confined region. For Hamiltonian models, recent works were focused on resonance-type phenomena, which were demonstrated in Ref. [4] to be responsible for very sharp and selective resonant transfer of energy between coupled dimers (a donor-acceptor pair). Another direction recently pursued in the studies of conservative systems is blocking, routing, and channeling of small-amplitude mobile discrete solitons by an array of large-amplitude strongly localized immobile ones [5].

In this work, we aim to explore a different but somewhat related possibility to manipulate solitons, which can be realized in a variety of physical systems. We will consider a model of a manipulating arm in the form of an ac driving force, localized at a moving spatial spot, with the objective to transfer a solitary pulse from an initial position to a target spot, in one- and two-dimensional (1D and 2D) cases. Possibilities to control the surface catalytic activity by laser beams [3], or affect local properties of a surface by the tip of a scanning tunneling microscope [6] are particular examples of a broad spectrum of systems where this scheme can be implemented. Other examples are the use of a transverse laser beam to switch spatial solitons in optical waveguides [7], and the use of narrow electron beams for sensing soliton states in long Josephson junctions [8]. The model considered in the present work may also be a step in the design of micromachines using laser beams as manipulating tools [9].

We will consider this possibility in a context that includes such ubiquitous features as dispersion, nonlinearity, and loss, leading through their interplay to the existence of solitons that may be supported by the ac drive. A fundamental model incorporating all these features is a damped nonlinear Schrödinger (NLS) equation, in both its continuum [10] and discrete [11] versions. The model will also include a spatially localized *mobile* ac driving force. The most straightforward experimental implementation of such a drive can be provided for by a laser or electron beam with a temporally modulated intensity. A continuum version of the model incorporating these ingredients is

$$iu_t + (1/2)u_{xx} + |u|^2 u = -i\gamma u + i\Gamma \operatorname{sech}[x - \xi(t)]\exp(it/2). \tag{1}$$

Here, $\gamma > 0$ is the loss coefficient, the frequency of the ac drive is normalized to be 1/2, and Γ is the strength of the sech-localized drive. The function $\xi(t)$ determines how the object (the soliton) is to be moved from an initial position, ξ_{in}, to the final one, ξ_{fin}; for instance,

$$\xi(t) = (1/2)[(\xi_{in} + \xi_{fin}) + (\xi_{fin} - \xi_{in})\tanh\tau], \tag{2}$$

where $\tau \equiv \epsilon t$ and ϵ is a small parameter setting the temporal scale of the arm's action. The model based on Eq. (1) neglects depletion of the driving field and its intrinsic spectral structure. For the actual sizes of the driven objects and small distances they should be moved across, both these assumptions can be easily justified.

The pulse dragged by the arm is sought for as a the unperturbed NLS soliton,

$$u_{sol}(x,t) = \eta \operatorname{sech}[\eta(x - \zeta(t)]\exp[i\phi(t) + i\dot\zeta\{x - \zeta(t)\}], \tag{3}$$

where η, $\phi(t)$, and $\zeta(t)$ are its amplitude, phase, and the position of its center, the overdot standing for the time derivative. In the first approximation, the soliton's phase

evolves according to the unperturbed equation $d\phi/dt = (\eta^2 + \dot{\zeta}^2)/2$. Note that the choice of the arm's width in Eq. (1) implies that the dragged soliton has $\eta \approx 1$. As we expect the soliton's position $\zeta(t)$ to follow the slow motion of the arm, which is described by $\xi(t)$, we define the lagging distance $\theta(t)$, along with a phase lag $\psi(t)$,

$$\theta(t) \equiv \zeta(t) - \xi(t), \quad \psi(t) \equiv \phi(t) - t/2. \tag{4}$$

Assuming that the parameters γ and Γ in Eq. (1) are small, evolution equations for the amplitude and velocity of the soliton can be derived by means of balance equations (BEs) [12] for the soliton's mass $M \equiv \int_{-\infty}^{+\infty} |u|^2 dx = 2\eta$ and momentum $P \equiv \int_{-\infty}^{+\infty} u u_x^* dx = 2\eta\zeta$. In particular, BE for the mass takes the form $d\eta/dt = -2\gamma\eta + 2\eta\Gamma(\theta/\sin\theta)\cos\psi$, where it was taken into account that $\eta \approx 1$. Adding BE for the momentum and making use of the evolution equation for the soliton's phase ϕ, we obtain

$$\frac{d^2\psi}{d\tau^2} + 2\epsilon\frac{d\psi}{d\tau} = -2g + 2G\frac{\theta}{\sin\theta}\cos\psi, \tag{5}$$

$$\frac{d^2\theta}{d\tau^2} + \epsilon G f_1(\theta)\frac{d\theta}{d\tau} = -\frac{d^2\xi}{d\tau^2} - \epsilon G f_1(\theta)\frac{d\xi}{dt} - G f_2(\theta)\sin\psi, \tag{6}$$

where $g \equiv \gamma/\epsilon^2$, $G \equiv \Gamma/\epsilon^2$, and

$$f_1(\theta) \equiv \int_{-\infty}^{+\infty} \frac{z\sinh z}{\cosh(z+\theta)\cosh^2 z} dz,$$

$$f_2(\theta) \equiv \int_{-\infty}^{+\infty} \frac{\sinh z}{\cosh(z+\theta)\cosh^2 z} dz.$$

If the arm is trying to move the soliton at a constant speed $V_0 \equiv d\xi/dt$, Eqs. (5) and (6) have two fixed-point (FP) solutions with small values of θ:

$$\psi = \pm\cos^{-1}(g/G), \quad \theta = \mp\frac{3}{2}\frac{\epsilon V_0}{\sqrt{1-g^2/G^2}}, \tag{7}$$

which implies that a necessary condition for the existence of the driven soliton is $g < G$. To analyze the stability of the FP solutions, Eqs. (5) and (6) are linearized around them for infinitesimal perturbations $\sim \exp(\sigma\tau)$, that gives rise to two equations which determine four eigenvalues σ:

$$\sigma^2 + 2\epsilon\sigma \pm 2\sqrt{G^2 - g^2} = 0, \quad \sigma^2 + \epsilon G\sigma \pm (2/3)\sqrt{G^2 - g^2} = 0. \tag{8}$$

It follows from Eqs. (7) that the FP (7) with the *upper* sign (i.e., negative θ) is a stable spiral, while the other solution is a saddle point. Hence, the stable state corresponds to the soliton *trailing behind* the arm, while the soliton pushed ahead of the arm is predicted to be unstable.

As is illustrated by Fig. 1, in direct simulations of the systems (1) and (2) we could easily observe, for very different values of the parameters, that the soliton is captured by
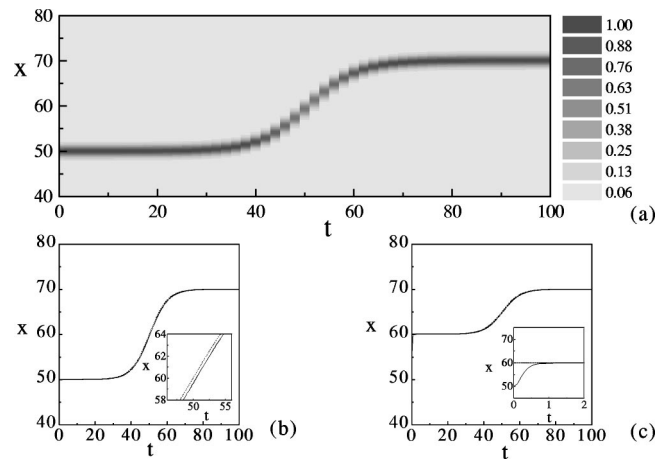
FIG. 1. (a) Gray-scale plot showing the evolution of the field intensity $|u(x,t)|^2$ in the driven solitons in the (x,t) plane. (b) Trajectories of the centers of the soliton (solid line) and driving arm (dashed line) when the soliton and the arm are initially centered at the same place, with $\xi_{\text{in}} = \zeta(t=0) = 50$, or (c) at different places, with $\xi_{\text{in}} = 60$, $\zeta(t=0) = 50$ [see the lower inset of (c)]. The inset of panel (b) shows a detail of the transport process indicating the lag between the preceding arm and the following soliton. The parameters are $\gamma = 1$, $\Gamma = 1.1$, and $\epsilon = \pi/20$, $\xi_{\text{in}} = 50$, and $\xi_{\text{fin}} = 70$.

the arm and dragged by it very robustly, even if the initial separation between the soliton and the arm is considerable [Fig. 1(c)]. As it is seen in Fig. 1(b), at the initial and final stages of the simulation, when the arm is quiescent, the soliton is at the same position as the arm (as predicted above); at the intermediate stage, when the arm moves at an approximately constant velocity, more careful analysis of the numerical data demonstrates that the soliton is slightly lagging behind the arm as expected. Despite the approximate nature of the theoretical calculation and the fact that the speed of the arm is not really constant, fairly good agreement is obtained between the theoretical (0.888) and numerical (0.792) values of the lag in Fig. 1(c).

In accordance with the prediction of the perturbation theory, the simulations demonstrate that the arm can support and drag the soliton in the lossy medium if its strength Γ exceeds a minimum value $\Gamma_{\min}$; for instance, $\Gamma_{\min} \approx 0.05$ if $\gamma = 1$; equivalently, for given Γ the loss constant must be smaller than a certain maximum value $\gamma_{\max}$; for example, $\gamma_{\max} \approx 1.24$ if $\Gamma = 1$. The numerical results also show that the soliton-transfer regime loses its stability if Γ exceeds a certain *maximum* value $\Gamma_{\max}$. In this case, the soliton does not follow the arm; instead its profile steepens and it emits wakes of radiation. For instance, $\Gamma_{\max}(\gamma = 1) \approx 2.96$. For given Γ, a related stability condition is that γ must exceed a *minimum* value γ_{cr}; for example, $\gamma_{\text{cr}}(\Gamma = 1) \approx 0.42$. Thus, the stable transfer regime occurs in an interval $\Gamma_{\min} < \Gamma < \Gamma_{\max}$ for fixed γ, or $\gamma_{\min} < \gamma < \gamma_{\max}$ for fixed Γ.

The same transport problem was also studied for the discrete version of Eq. (1),

$$i(du_n/dt) + (1/2)\Delta_2 u_n + |u_n|^2 u_n$$
$$= -i\gamma u_n + i\Gamma\,\text{sech}[nh - \xi(t)]\exp(it/2), \tag{9}$$
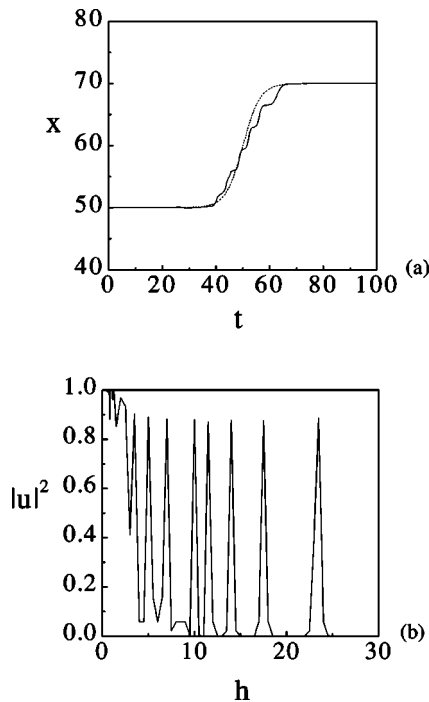
FIG. 2. (a) Trajectories of the centers of the soliton (solid line) and driving arm (dashed line) in the discrete model with the spacing $h=2$ for the same values of other parameters as in Fig. 1. (b) The field intensity at the center of the soliton at $t=100$ vs the lattice spacing h.

where h is the spacing of the lattice, and $\Delta_2 u_n \equiv (u_{n+1} + u_{n-1} - 2u_n)/h^2$ accounts for the coupling between the adjacent sites. In the discrete case, which is relevant to a number of contexts such as optical lattices in Bose-Einstein condensates (see, e.g., Ref. [13]) and coupled arrays of optical waveguides [14], stable transfer of the discrete soliton by the arm was found too. As is well known [15] (see also Ref. [11]), in nonintegrable dynamical lattices a soliton generically encounters a potential-energy (Peierls-Nabarro) barrier. Accordingly, the motion of the driven discrete soliton resembles the saltatory propagation of "lurching waves" [16]. Nevertheless, it relaxes to the prescribed target position even if the discreteness is *very strong*, as is seen in Fig. 2(a). This result is in contrast with the well-known phenomenon of propagation failure [15] in the case of the free motion of solitons in lattices.

Another noteworthy feature of the discrete problem is observed if the amplitude of the pulse delivered to the target position is considered vs the lattice spacing h, to quantify the effects of discreteness. Peaks in Fig. 2(b) clearly indicate the presence of a resonance mechanism affecting the pulse transport in the lattice. In fact, this mechanism was predicted analytically and numerically in a number of theoretical works [17] and observed experimentally in lattices [18] and quasilattices (periodically modulated continua) [19]. Namely, the lattice spacing h and a given driving-arm's velocity V_0 define the frequency $2\pi V_0/h$ of the periodic passage of the lattice site by the soliton, which can resonate with the ac-drive's frequency ω_0. In the case when the arm moves according to Eq. (2), the nearly constant velocity of the arm in
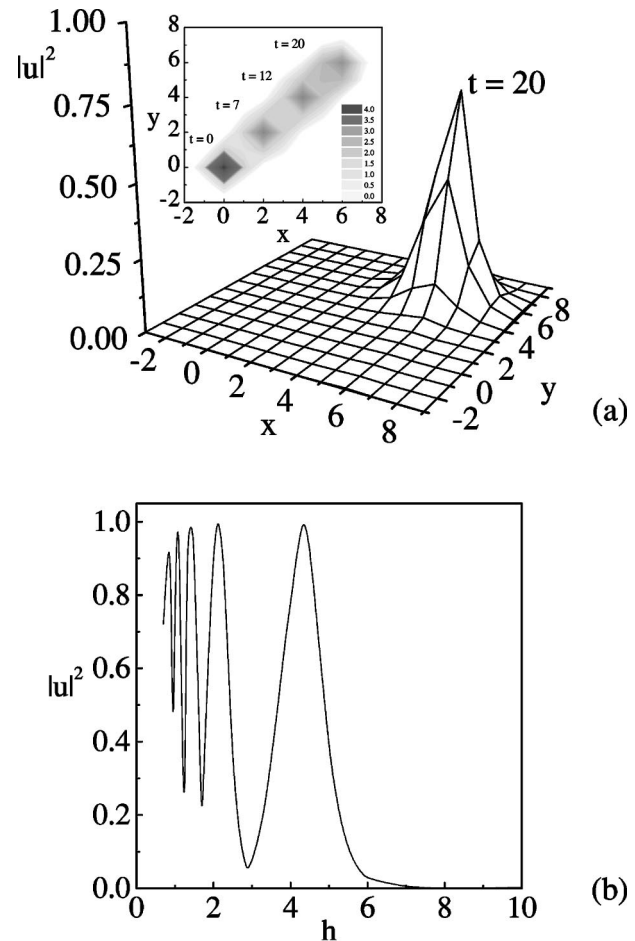
FIG. 3. (a) A set of contour-plot traces illustrating the evolution of the pulse in the 2D lattice with $\gamma = \Gamma = 1$ and $h = 2$, which is transferred from $x_{in} = y_{in} = 0$ to the target position at $x_{fin} = y_{fin} = 5$. The soliton in the eventual position is shown explicitly; obviously, it well preserves the shape. (b) The field intensity at the center of the 2D soliton, in its final position vs the lattice spacing, cf. Fig. 2(b).

the interval $|t| \lesssim \epsilon^{-1}$ is $V_0 \approx (\epsilon/2)(\xi_{fin} - \xi_{in})$. Since we have $\omega_0 \equiv 1/2$ in Eq. (1), the resonance condition is

$$h = 4\pi V_0/m, \qquad (10)$$

where m is a positive integer (resonance order). These resonances are identified in Fig. 2(b), except for the one corresponding to $m=1$. For instance, Eq. (10) predicts the $m=2$ resonance, in the case examined ($\epsilon = \pi/20, \xi_{fin} - \xi_{in} = 20$), at $h = \pi^2$, while the simulations reveal a resonance at $h \approx 10$. In all the cases examined, with $m = 2,3,4, \ldots$, a relative discrepancy between the theoretically predicted and numerically found positions of the resonance was $<3\%$, and in most cases it was close to 1%. The residual discrepancy may be due to the finite precision the numerical experiments and the approximate nature of the resonance condition, given that the arm's speed is not exactly constant; see Eq. (2). Interestingly, not only the resonances of integer orders, but also fractional resonances were found, satisfying the condition $h = 4\pi V_0(l/m)$, with an integer $l \neq 1$. For example, the maxi-

mum resonant value of h in Fig. 2(b) corresponds to the fractional resonance at $m/l = 5/9$, the next one to $m/l = 6/7$, and so on, with accuracy of $\approx 1\%$.

To further illustrate the generality and robustness of the proposed mechanism, we also examined the possibility of targeted transfer of solitons in the 2D case. In this case, the continuum NLS equation with the cubic nonlinearity is subject to wave collapse [10]. We focus here on the 2D NLS lattice model with cubic nonlinearity, which readily gives rise to stable solitons, provided that the lattice spacing exceeds a critical value [11,20]. In the latter case, Eq. (9) becomes

$$
\begin{aligned}
i(du_{mn}/dt) + (1/2)\Delta_2 u_{mn} + |u_{mn}|^2 u_{mn} \\
= -i\gamma u_{mn} + i\Gamma \, \text{sech}[\sqrt{m^2 + n^2}\, h - \xi(t)]\exp(it/2),
\end{aligned}
\tag{11}
$$

where

$$
\Delta_2 u_{mn} \equiv (u_{m,n+1} + u_{m,n-1} + u_{m+1,n} + u_{m-1,n} - 4u_{m,n})/h^2.
$$

In the simulations, we started with those stable solitons in the unperturbed model, constructed by means of the Newton method [20]. The discrete pulse is then transferred by the localized arm to a predetermined destination in the 2D lattice. Results, a typical example of which is displayed in Fig. 3(a), are generic, in the sense that the arm always delivers the soliton to the target point, which may be expected since the transfer is essentially occurring in an effectively 1D way (radially) along the lattice. Resonances similar to those found above in the 1D case [(Fig. 2(b)], for the amplitude of the transported pulses as a function of h can also be readily found in the 2D case, see Fig. 3(b).

In summary, we have demonstrated a mechanism for coherent transfer of solitary waves from an original position to a specified target position. The mechanism has been demonstrated, analytically and numerically, in continuum and lattice media, in both one and two spatial dimensions. Fairly broad parameter regions in which the mechanism is stable were identified. In the lattice medium, the analysis and simulations reveal that the stable operation of the soliton-driving arm is determined by the resonant energy transfer from the ac drive to the solitary wave, both integer and fractional resonances being well pronounced.

---

[1] Y. Kuramoto, *Chemical Oscillations, Waves and Turbulence* (Springer-Verlag, Berlin, 1984).

[2] E. Infeld and G. Rowlands, *Nonlinear Waves, Solitons, and Chaos* (Cambridge University Press, Cambridge, UK, 2000).

[3] J. Wolff, A.G. Papathanasiou, I.G. Kevrekidis, H.H. Rotermund, and G. Ertl, Science **294**, 134 (2001).

[4] G. Kopidakis, S. Aubry, and G.P. Tsironis, Phys. Rev. Lett. **87**, 165501 (2001).

[5] D.N. Christodoulides and E.D. Eugenieva, Phys. Rev. Lett. **87**, 233901 (2001).

[6] *Scanning Tunneling Microscopy III: Theory of STM and Related Scanning Probe Methods*, edited by R. Wiesendanger and H.-J. Güntherodt (Springer-Verlag, Berlin, 1993).

[7] B.A. Malomed *et al.*, J. Opt. Soc. Am. B **16**, 1197 (1999); B. Gisin *et al.*, Phys. Rev. E **62**, 2804 (2000).

[8] S.G. Lachenmann *et al.*, J. Appl. Phys. **77**, 2598 (1995); A. Laub *et al.*, Phys. Rev. Lett. **75**, 1372 (1995); A.V. Ustinov and B.A. Malomed, Phys. Rev. B **54**, 9047 (1996).

[9] P. Galajda and P. Ormos, Appl. Phys. Lett. **78**, 249 (2001).

[10] C. Sulem and P. L. Sulem. *The Nonlinear Schrödinger Equation* (Springer-Verlag, New York, 1999).

[11] P.G. Kevrekidis, K.Ø. Rasmussen, and A.R. Bishop, Int. J. Mod. Phys. B **15**, 2833 (2001).

[12] Y.S. Kivshar and B.A. Malomed, Rev. Mod. Phys. **61**, 763 (1989).

[13] A. Trombettoni and A. Smerzi, Phys. Rev. Lett. **86**, 2353, (2001); F. Kh. Abdullaev *et al.*, Phys. Rev. A **64**, 043606 (2001).

[14] D.N. Christodoulides and R.I. Joseph, Opt. Lett. **13**, 794 (1988).

[15] M. Peyrard and M. Kruskal, Physica D **14**, 88 (1984).

[16] D.H. Terman, G.B. Ermentrout, and A.C. Yew, SIAM (Soc. Ind. Appl. Math.) J. Appl. Math. **61**, 1578 (2001), and references therein.

[17] L.L. Bonilla and B.A. Malomed, Phys. Rev. B **43**, 11 539 (1991); B.A. Malomed, Phys. Rev. A **45**, 4097 (1992); T. Kuusela *et al.*, J. Phys. A **26**, L21 (1993); G. Filatrella and B.A. Malomed, J. Phys.: Condens. Matter **11**, 7103 (1999).

[18] T. Kuusela, Phys. Lett. A **167**, 54 (1992).

[19] A.V. Ustinov and B.A. Malomed, Phys. Rev. B **64**, 020302(R) (2001).

[20] P.G. Kevrekidis, K.Ø. Rasmussen, and A.R. Bishop, Phys. Rev. E **61**, 2006 (2000).